Structures of hypo-, and hyper-stoichiometric $UO_{2\pm x}$ doped with Trivalent Rare Earth.

Jandee Kim[a], Jeongmook Lee[a], Young-Sang Youn[a], Nazhen Liu[b], Jong-Goo Kim[a], Yeong-Keong Ha[a], Sang-Eun Bae[a], David W. Shoesmith and Jong-Yun Kim[a,*]
[a]*Department of Nuclear Chemistry Research, KAERI, Daejeon, 34057, Korea*
[b]*Department of Chemistry,Western University, London, Ontario N6A 5B7, Canada*
kimjd@kaeri.re.kr

1. Introduction

The model calculations of a loss of container wall thickness by general corrosion have shown that only a few microns of container failure occurs [1-2]. However, it can be assumed that some containers will fail allowing groundwater to contact the fuel causing radionuclide release. Because the major radio nuclides are located within the oxide matrix, their release rates to the groundwater will be depended on the fuel corrosion/dissolution rate. The key factors to determine the UO_2 dissolution behaviors, can control the reactivity of the UO_2 matrix, are (i) stoichiometry of $UO_{2\pm x}$ matrix; (ii) rare earth (RE) element doping in UO_2 matrix; and (iii) environmental condition including chemical composition and pH of water to contact with [3-5].

Because spent nuclear fuel is consisted with stoichiometric UO_2, and also parts of hypo-, and hyper-stoichiometric $UO_{2\pm x}$ matrix, it is important to comprehend chemical and physical properties of matrix depend on differential stoichiometry from dissolution behavior, which determine the release of radionuclides [6-8]. H. He and D.W. Shoesmith reported that local corrosion kinetics of hyper-stoichiometric UO_{2+x} were determined by using SECM approach curves in the presence of oxidant at the corrosion potential [7-8].

Also, the influence of fission products including RE (Rare earth) element on the oxidation of UO_2 has been investigated [9-11]. UO_2 has been studied extensively in order to determine the effect of fission-product impurities present in solid solution in used fuel. Due to their presence, enhance the stability of the cubic fluorite structures of U_4O_9-type with respect to U_3O_8-type depending on the sintering atmoshpere as compared to un-doped UO_2 [12-13]. Ho and Radford reported that charge compensation in the Gd doped urania can be described with formation of oxygen vacancy, oxidation of U^{4+} to U^{6+} via U^{5+}, interstitial formation or combination of defect types [14].

In determining fuel dissolution and radionuclide release rates, the reactivity of the UO_2 matrix and how it is modified by prior irradiation, is important. The one of the important changes expected to influence the reactivity of the fuel is the rare earth doping of UO_2 which will change the conductivity and structural properties of the UO_2 matrix.

This work presents hypo-, and hyper-stoichiometric $UO_{2\pm x}$, and/or low and highly doped $U_{1-y}Gd_yO_{2\pm x}$ manufactured by mechanical blending method followed by oxidation with control the oxygen potential. Stoichiometry of all pellets was determined and distinguished into hypo-, and hyper-stoichiometric $UO_{2\pm x}$ by analysis of using non-distructive X-ray method, conveniently. And influences of non-stoichiometric urania matrix and Gd dopant on dissolution behaviors of $UO_{2\pm x}$ matrix were investigated by electrochemical study.

2. Methods and Results

2.1 Preparation of $U_{1-y}Gd_yO_{2\pm x}$ pellets

The un-irradiated UO_2 and Gd doped UO_2 pellets are fabricated by sintering pressed green pellets at ~1700 ºC in a reducing atmosphere, which are prepared by blending method to grain UO_2 powders and/or Gd_2O_3 containing UO_2 powders followed pressing with 300 MPa. The doped Gd amounts were 5 and 10 mol% contrasting with uranium, respectively. All green pellets were weighed before and after sintering process to estimate additional or missing oxygen. Pellets were sintered on alumina crucible in a linear type of furnace at 1700ºC in a reducing atmosphere of Ar-4 % of H_2 for 24 hrs. Because hypo-stoichiometric UO_{2-x} was manufactured by this reducing condition, hyper-stoichiometry was adjusted by followed mild oxidation step control the oxygen potential by CO/CO_2 mixed gas ratio from 10 to 0.001, temperatures and Gd contents (mol%), according to the Ellingham diagram. Prepared pellets have ~8 mm dia. and less than 1 mm thickness.

2.2 Grain structure of non-stoichiometric UO_2

Scanning electron microscopy (model No., Jeol, USA) results, using 20 keV electron acceleration voltage with 10 mm of working distance, revealed morphological evolutions and grain features of freshly prepared pellet depending on Gd-doped level and stoichiometry.

Highly densed pellets were produced by sintering the pellets at 1700 ˚C in hydrogen mood for 18 hrs after pressed UO_2 powder which containing 5 and 10 mol% of Gd dopants. Interesting point is that sintered Gd

doped UO_2 pellets have curvatures looked like arch shapes as much as increase the Gd doped amounts. In addition, the grain structures changed drastically depend on Gd-doped level as shown in Figure 1. In case of un-doped hypo-stoichiometric UO_{2-x} (Figure 1(a)), it has polygonal structures consisted of wrinkled and flattened domains, are observed ~5 to ~15 μm sized, and the domain size decreases rapidly with increase of Gd doping level (Figure 1(b-c)). On the other hand, hyper-stoichiometric pellets prepared by through the CO/CO_2 oxidation of hypo-stoichiometric pellets, have more big domains of over 20 um sized as shown in Figure 1(d). Hyper-stoichiometric UO_{2+x} present more large sized (over 20 μm) and smooth textured grains as shown in Figure 1(d). The interstitial oxygen activates internal strain of distorted cubic lattice, followed by enhanced uranium diffusion results in crystalline growths. H. He and D. W. Shoesmith demonstrate diverse features of $UO_{2\pm x}$ grains on stoichiometric UO_2 pellet, and hyper-stoichiometric one, respectively. Hyper stoichiometric $UO_{2.1}$ pellet has inhomogeneous stoichiometric distributions of domains consisted of various O/U values from 1.96 to 2.32, possess smooth and polygonal features. They explained that the distribution of excess O^{2-} makes to develop domain growth affects to domain structures of various size, texture and figurations.

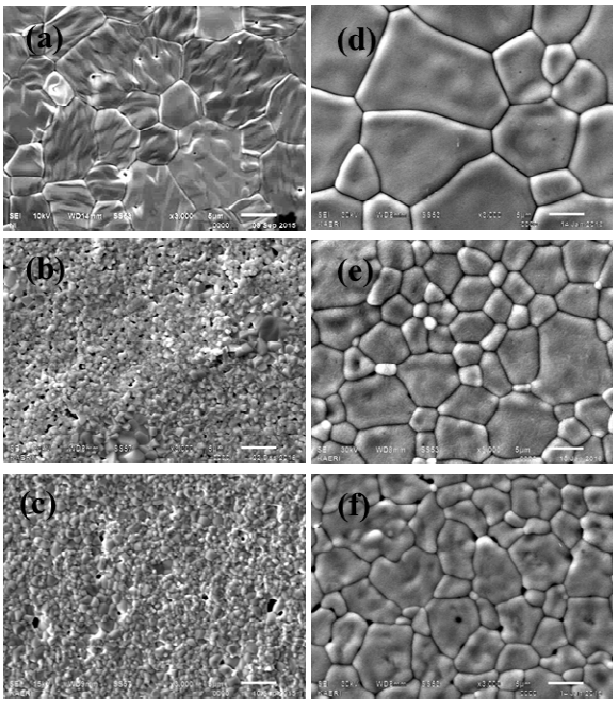

Fig. 1 Structural changes of grains on as prepared (a-c) hypo-stoichiometric; and (d-f) hyper-stoichiometric $U_{1-y}Gd_yO_{2\pm x}$ depend on Gd contents which are (a,d) 0; (b,e) 5; and (c,f,) 10 mol%. Magnifications of SEM images are ×3000, and scale bar represents 5 μm length.

2.3 Lattice parameters

The phase present were identified by X-ray diffraction (D8 ADVANCE, Bruker, USA), using Cu K_α radiation, and the lattice parameters of the fluorite matrix was calculated from high Bragg-angle reflections (in the 2θ range of 20˚ to 120˚) using TOPAS (Version 4.2, Bruker AXS) analysis software.

In actual fabrication of uranium based fuels, which can be slightly hyper-stoichiometric induce lattice contraction. Therefore, obtaining proper stoichiometry is essential to determine the lattice dependency in function of the concentration of dopant. Figure 2 shows lattice parameters of $U_{1-y}Gd_yO_{2\pm x}$ depending on Gd-doped mol% (y) from X-ray diffraction analysis. Stoichiometric $U_{1-y}Gd_yO_2$ presented with dashed line, in which the lattice parameter decreases with increase of Gd doping contents up to 10 mol%. This shows linear correlation depend on doped Gd molar percent, with slope value of -0.0173 which is reasonable contraction factor of stoichiometric $U_{1-y}Gd_yO_2$ in the range of extensively published for decades. Because Gd_2O_3 can be considered as a fluorite-type structure, Gd doped UO_2 can form a cubic fluorite-type structure in stoichiometric UO_2 with ease. And charge compensation in the Gd-doped UO_2 can be realized by forming vacancy cluster, oxidation of U^{4+} to U^{6+} via U^{5+}, interstitial formation or a combination of these defect types, depending on O/U ratio.

In case of hyper-stoichiometric pellets (x>0), show the most steep slope of lattice change in Figure 2 (x>0). Because U^{5+} ratio in UO_{2+x} matrix increases due to interstitial oxygen anion in hyper-stoichiometry, and U^{5+} (0.88 Å) is smaller than U^{4+} (1.001 Å). Therefore, the lattice parameter decreases which can be presented with linearity of eq (1), even though relatively large Gd^{3+} (1.053 Å) ions are introduced.

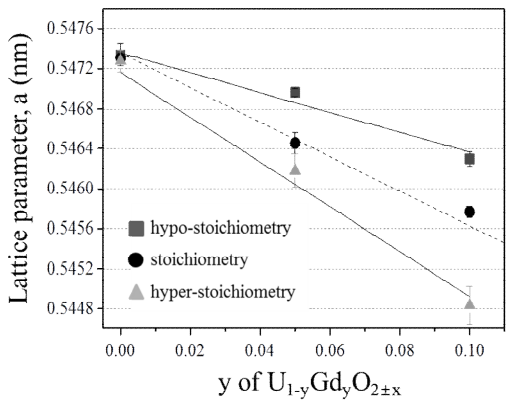

Fig.2 Lattice contractions of hypo-, and hyper-stoichiometric Gd-doped $UO_{2\pm x}$ as a function of molar fraction of doped Gd, y, and dashed line demonstrates varying the lattice parameter of stoichiometric Gd-doped UO_2 depends on doping fraction

In contrast, hypo-stoichiometric $U_{1-y}Gd_yO_{2-x}$ in which the lattice parameter presents more gradual slope of -0.00995, than hyper- and stoichiometric ones as shown in Figure 2. Ohmichi et al. explained that hypo-stoichiometry possess increasing of oxygen vacancy in

which is 10% larger than that of the O^{2-} ion, leads on volumetric expansion as comparing with stoichiometric or hyper-stoichiometric $U_{1-y}Gd_yO_{2+x}$ [15].

On the other hand, 5 and 10 mol% Gd-doped $U_{1-y}Gd_yO_{2+x}$ have shown somewhat big standard deviation as comparing with hypo-stoichiometric pellets and un-doped ones. This might be caused by un-homogeneously distributed Gd in solid solutions of hyper-stoichiometric pellets, results in observation of partially different lattice parameters on surface of pellets.

3. Conclusion

Non-stoichiometric Gd-doped UO_2 pellets are prepared by mechanical blending method which sinter the green pellets with control the oxygen potential. Hyper-stoichiometric pellets have shown the tolerance to retain grain size though Gd dopants increase, due to interstitial oxygen ions in UO_{2+x} matrix, which allows improvement of uranium diffusion in solid solution. And the lattice contraction of pellets was observed to determine the stoichiometry conveniently, depend on Gd contents and stoichiometry. Gd doped in hyper-stoichiometric $U_{1-y}Gd_yO_{2+x}$ shows more dramatic contraction of lattice parameter depend on Gd contents, according to formation of smaller sized U^{5+} in matrix, even though Gd^{3+} are introduced. Meanwhile, larger oxygen vacancy in hypo-stoichiometry induces volumetric expansion.

Acknowledgment

This work supported by the National Research Foundation of Korea (NRF) grant funded by the Korea government (MSIP) (No. 2012M2A8A5025925)

References

[1] A. C. Fraker, Corrosion of zircaloy spent fuel cladding in a repository NIST Report: NISTIR 89-4114 1989.
[2] L. H. Johnson, F. King, Canister Options for the Disposal of Spent Fuel, Technical report of Nagra (2003) 02-11.
[3] R. J. McEachern, D. C. Doern, and D. D. Wood, J. Nucl. Mater. 252 (1998) 145-149.
[4] L. E. Thomas, R. E. Einziger, and H. C. Buchanan, J. Nucl. Mater. 201 (1993) 310-319.
[5] K. Park and D. R. Olander, J. Nucl. Mater. 187 (1992) 89-96.
[6] R.J. McEachern, P. Taylor, J. Nucl. Mater. 254 (1998) 87–121.
[7] H. He, R.K. Zhu, Z. Qin, P. Keech, Z. Ding, D.W. Shoesmith, J. Electrochem. Soc. 156 (2009) C87-C94.
[8] H. He, Z. Qin, D.W. Shoesmith, Electrochim. Acta 56 (2010) 53-60.
[9] H. He, P.G. Keech, M.E. Broczkowski, J.J. Noel, D.W. Shoesmith, Can. J. Chem. 85 (2007) 702-713.
[10] H. He, R.K. Zhu, Z. Qin, P. Keech, Z. Ding, D.W. Shoesmith, J. Electrochem. Soc. 156 (2009) C87-C94.
[11] H. He, Z. Qin, D.W. Shoesmith, Electrochim. Acta 56 (2010) 53-60.
[12] R.J. McEachern, D.C. Doern, D.D. Wood, J. Nucl. Mater. 252 (1998) 145-149.
[13] L.E. Thomas, R.E. Einziger, H.C. Buchanan, J. Nucl. Mater. 201 (1993) 310-319.
[14] S.M. HO, K.C. Radford, Nucl. Technol. 73 (1986) 350-360.
[15] T. Ohmichi, S. Fukushima, A. Maeda, H. Watanabe, J. Nucl. Mater. 102 (1981) 40-46.